ELSEVIER

Biochemical Pharmacology 65 (2003) 161–172

Biochemical Pharmacology

Pyridoxal isonicotinoyl hydrazone analogs induce apoptosis in hematopoietic cells due to their iron-chelating properties

Joan L. Buss[a], Jiri Neuzil[b,c,1], Nina Gellert[c], Christian Weber[c,d], Prem Ponka[a,*]

[a]*Departments of Physiology and Medicine, McGill University, and Lady Davis Institute for Medical Research, Sir Mortimer B. Davis Jewish General Hospital, 3755 chemin de la Cote-Ste-Catherine, Montreal, Que., Canada H3T 1E2*
[b]*Division of Pathology II, Faculty of Health Sciences, University Hospital, Linköping, Sweden*
[c]*Institute for Prevention of Cardiovascular Diseases, Ludwig Maximilians University, Munich, Germany*
[d]*Department of Cardiovascular Molecular Biology, University Hospital, Aachen, Germany*

Received 5 December 2001; accepted 13 June 2002

Abstract

Analogs of pyridoxal isonicotinoyl hydrazone (PIH) are of interest as iron chelators for the treatment of secondary iron overload and cancer. PIH, salicylaldehyde isonicotinoyl hydrazone (SIH), and 2-hydroxy-1-naphthylaldehyde isonicotinoyl hydrazone (NIH), the toxicity of which vary over two orders of magnitude, were selected for a study of their mechanisms of toxicity. PIH analogs and their iron complexes caused concentration- and time-dependent apoptosis in Jurkat T lymphocytes and K562 cells. Bcl-2 overexpression was partially anti-apoptotic, suggesting mitochondrial mediation of apoptosis. Since the pan-caspase inhibitor zVAD-fmk did not reduce lysosomal and mitochondrial destabilization, these events occur upstream of caspase activation. In contrast, phosphatidylserine externalization and the development of apoptotic morphology were inhibited significantly, indicating the role of caspases in mediating these later events. Since overexpression of CrmA had no effect on apoptosis, caspase-8 is not likely involved. Fe^{3+} complexes of SIH and NIH, which accumulated in ^{59}Fe-labeled mouse reticulocytes during incubation with the chelators, also caused apoptosis. BSA, which promotes release of the complexes from cells, reduced the toxicity of SIH and NIH, suggesting that the induction of apoptosis by PIH analogs involves toxic effects mediated by their Fe^{3+} complexes. Moreover, analogs of these agents lacking the iron-chelating moiety were non-toxic.

Keywords: Apoptosis; Pyridoxal isonicotinoyl hydrazone; Jurkat; K562; Iron chelators

1. Introduction

Iron is essential for life due to its roles in oxygen transport and one-electron redox chemistry. Complex mechanisms have evolved to allow delivery of iron to tissues [1], which prevent it from acting as a catalyst for the production of reactive oxygen species that damage cell membranes, nucleic acids, and proteins. Excretion of iron is limited to cell desquamation, as there is no specific pathway by which it is eliminated. Iron homeostasis in the organism depends upon efficient recycling of its body stores and tightly controlled intestinal absorption. When iron intake exceeds the requirements of the organism, as is the case for hereditary hemochromatosis and secondary iron-overload disorders, it gradually accumulates in the parenchyma. When the capacity to safely store iron in ferritin is exceeded, the target organs, namely the liver, kidney, and heart, begin to exhibit pathophysiology characteristic of iron overload. The observed toxicity of iron is thought to be due to iron-based oxidative stress. There is increasing evidence that iron may play a role in the pathophysiology of numerous conditions in individuals who are not iron-overloaded, including ischemia/reperfusion injuries such as

* Corresponding author. Tel.: +1-514-340-8222, Ext. 5289; fax: +1-514-340-7502.
E-mail address: prem.ponka@mcgill.ca (P. Ponka).
[1] Present address: Heart Foundation Research Center, School of Health Sciences, Griffith University, Southport, Queensland, Australia.

Abbreviations: AO, acridine orange; BBH, benzaldehyde benzoyl hydrazone; BIH, benzaldehyde isonicotinoyl hydrazone; DFO, desferrioxamine; FBS, fetal bovine serum; IRP, iron regulatory protein; MSDH, *O*-methylserine dodecylamide hydrochloride; MTS, 3-(4,5-dimethylthiazol-2-yl)-5-(3-carboxymethoxyphenyl)-2-(4-sulfophenyl)-2*H*-tetrazolium; NIH, 2-hydroxy-1-naphthylaldehyde isonicotinoyl hydrazone; PIH, pyridoxal isonicotinoyl hydrazone; SIH, salicylaldehyde isonicotinoyl hydrazone.

0006-2952/02/$ – see front matter © 2002 Published by Elsevier Science Inc.
PII: S0006-2952(02)01512-5

stroke and myocardial infarction, inflammatory diseases, and cancer. Although iron chelators are used to treat secondary iron overload, they have not been studied extensively as therapeutic agents to treat free radical-mediated tissue damage, despite their potential value.

Secondary iron-overload disorders, such as β-thalassemia, are caused by the hyperabsorption of iron and chronic blood transfusions, which are required as a source of functional erythrocytes. Concomitant chelation therapy is required for these patients to prevent liver and cardiac dysfunction, which occur by the age of 25 in the absence of iron-chelation therapy. At present, the only clinically accepted drug for this purpose is DFO which, due to its dosage form, is costly and inconvenient. There is, therefore, an ongoing search for an orally available iron-chelator, which would result in its accessibility to a greater number of patients.

In biological systems, iron chelators have multiple effects, which may or may not contribute to their effectiveness and/or toxicity. An improved understanding of the properties required of effective chelators will improve the screens for identification of therapeutically valuable compounds. Several iron chelators have been shown to induce apoptosis [2–6]. Iron chelators have many biological effects, which may result in apoptotic cell death, including inhibition of ribonucleotide reductase, redistribution of cellular iron, and formation of iron complexes that cause oxidative stress.

PIH is among the most effective orally available iron chelators known. It effectively causes iron excretion in humans [7] and rats [8], demonstrating its capacity to access biological iron rapidly. These effects were observed at doses that caused no significant adverse effects, and were well below LD_{50} values established in rats [9]. *In vitro* [10,11] and *in vivo* [12] studies have identified analogs that are far more effective than PIH itself. Previous studies have also demonstrated that the factors governing the toxicity of these chelators, which varies over two orders of magnitude [10], are complex and do not depend simply on the amount of iron mobilized [13]. Thus, PIH and its analogs warrant further study as a class of iron chelators that may be of value in treating diseases in which iron plays a significant role.

2. Materials and methods

2.1. Synthesis of BIH and BBH

BIH and BBH were synthesized using the general method previously described [14]. Briefly, 0.01 mol benzaldehyde and 0.01 mol isonicotinoyl or benzoyl hydrazide (all from Lancaster) were dissolved in 175 mL of 66% aqueous ethanol, refluxed for 30 min, cooled, filtered, and washed with water to yield BIH and BBH, respectively. BIH was recrystallized from ethanol. The identities and purities of both compounds were established by ^{1}H NMR. Stock solutions of 2 mM were made in RPMI-1640 medium containing 10% FBS and stored at −20° until used.

2.2. Preparation of chelators and their Fe^{3+} complexes

PIH, SIH, and NIH were prepared as previously described [14]. Stock solutions of 5 or 10 mM were prepared in 50 or 100 mM NaOH, and stored at −20° until used. Storage under these conditions did not result in significant hydrolysis over 6 months. Fe^{3+} complexes of the chelators were prepared at a minimum concentration of 25 μM by the addition of 5 mM $FeCl_3$ (Fisher) in 100 mM sodium citrate (Bioshop) and chelator in a 1:2 molar ratio, and incubated at room temperature for 60 min. Chelator stability under the storage conditions described and complex formation with Fe^{3+} were assessed at 25 and 37° using a Cary 1 spectrophotometer.

2.3. Cell culture

Jurkat T lymphoma cells, their mutants overexpressing Bcl-2 [15] or CrmA [16], and K562 cells were maintained in RPMI-1640 medium supplemented with 10% FBS. Anti-Fas IgM (Immunotech) was used at 20 ng/mL to induce apoptosis in control and Bcl-2- and CrmA-overexpressing Jurkat cells.

2.4. Cell toxicity experiments

K562 and Jurkat T cells were cultured in phenol red-free RPMI-1640 medium (Cellgro) supplemented with 10% FBS (Gibco) and 2 mM glutamine (Gibco). K562 or Jurkat cells from log phase cultures were plated in 96-well plates at 14,000 or 20,000 cells/well, respectively, in a final volume of 200 μL/well. Cell numbers were assessed using either trypan blue staining or the MTS assay (Promega). In the latter assay of mitochondrial dehydrogenase activity, phenomethazine sulfonate (Aldrich) mediates the reduction of MTS by cells to a compound that can be detected spectrophotometrically. Absorbance measurements were made at 490 nm, and corrected for background absorbance at 630 nm, on an EL_x800 microplate reader (Bio-tek Instruments) and, when necessary, were corrected for the absorbance of the iron-chelator complexes. Calibration curves of both cell types were linear over the range used in the toxicity experiments described, and treatment of cells with the chelators did not affect MTS reduction (data not shown). This was also the case for the treatment of Jurkat cells with iron complexes. Treatment of K562 cells with iron-chelator complexes appears to enhance their capacity to reduce MTS, since absorbance measurements were much higher than expected based on cell number [17]. For this reason, the toxicity of iron-chelator complexes toward K562 cells was not assessed in this study.

2.5. Mobilization of ^{59}Fe from mouse reticulocytes

Reticulocyte-enriched mouse blood labeled with ^{59}Fe was prepared. Briefly, reticulocytosis was induced in CD1 mice by intraperitoneal injection of 50 mg/kg of phenylhydrazine on three consecutive days, and blood was collected 3 days after the last injection. A 30% cell suspension was incubated in 1 mM succinylacetone, which inhibits heme biosynthesis, at 37° for 30 min, at which time 10 μM human $^{59}Fe_2$-transferrin (Sigma) [18] was added, and the incubation continued for 60 min. Cells were washed, and the total ^{59}Fe taken up by the cells was measured by γ-counting, corresponding to 100% ^{59}Fe. Packed cells (35 μL) were incubated with the chelators in a final volume of 500 μL MEM for 2 hr. Cells were centrifuged, and the total radioactivity in the supernatants was calculated by γ-counting small samples to determine the amounts of ^{59}Fe released from the cells. Cells were washed and lysed osmotically by the addition of 200 μL of distilled water. Intracellular ^{59}Fe in ethanol-soluble forms was separated from protein-associated ^{59}Fe by the precipitation of proteins using 1 mL of ice-cold ethanol, and the total radioactivity in both fractions was γ-counted. Thus, binding of ^{59}Fe by the chelators (the sum of ^{59}Fe in the supernatant and the ethanol-soluble fraction), and release of the resulting ^{59}Fe-chelator complexes from the cells (^{59}Fe in the supernatant) were measured. Under these conditions, cell viability in the presence of PIH analogs at concentrations of 50 μM was over 90% for all treatments, as assessed by the absence of hemoglobin release into the extracellular medium.

2.6. Assessment of apoptotic markers

Cells were seeded at 0.5×10^6/mL in RPMI medium containing 10% FBS and treated as indicated. Phosphatidylserine externalization, loss of the inner mitochondrial membrane potential ($\Delta\Psi_m$), and lysosomal destabilization were assessed by flow cytometry as described below.

Phosphatidylserine externalization was measured by the binding of annexin-V-FITC (PharMingen) [19]. Briefly, cells were washed in PBS, resuspended in binding buffer (10 mM HEPES/NaOH, pH 7.4, 140 mM NaCl, 2.5 mM $CaCl_2$), incubated for 20 min at room temperature with 2 μL annexin-V-FITC, and analyzed by flow cytometry using a FACScan instrument (Becton Dickinson), which measures the fluorescence intensity of individual cells. Since a small percentage of the control cells were highly fluorescent, the gating was set to encompass the approximately 95% of cells in the low-fluorescence peak. Cells with fluorescence above this range were considered apoptotic.

The mitochondrial inner membrane potential ($\Delta\Psi_m$) was assessed using 5,5′,6,6′-tetrachloro-1,1′,3,3′-tetraethylbenzimidazolyl-carbocyanine iodide (JC-1, Molecular Probes) [20]. Cells were washed, incubated with 10 μM JC-1 in RPMI medium for 15 min at 37°, washed with PBS, and analyzed by flow cytometry. The lysosomal stability assay was performed using the weak base AO as described [19]. Cells were washed and resuspended in 2.5 mL RPMI medium with 10 mM HEPES and 5 μg/mL of AO, incubated at 37° for 15 min in the dark, washed, and resuspended in PBS; the loss of red fluorescence was estimated using flow cytometry. Flow cytometric data measuring mitochondrial destabilization ($\Delta\Psi_m$) using JC-1 and lysosomal destabilization using AO were analyzed similarly to the annexin-V data. For both $\Delta\Psi_m$ and lysosomal destabilization, chelator treatment resulted in a loss of fluorescence as compared with controls. The gate was set on the control cells, and cells with fluorescence below this range were defined as having "low $\Delta\Psi_m$" or "pale" lysosomes for these assays, respectively.

Caspase-3 activity was measured essentially as published elsewhere [21]. In brief, 10^6 cells were lysed in 100 μL lysis buffer (10 mM Tris–HCl, pH 7.4, 130 mM NaCl, 0.1% Triton X-100, 10 mM NaH_2PO_4), mixed with 900 μL reaction buffer (20 mM HEPES, pH 7.4, 10% glycerol, 2 mM dithiothreitol), and incubated for 2 hr at 37° with the substrate for caspase-3, Ac-DEVD-AMC (Calbiochem), at a concentration of 50 μM. The fluorescence of the liberated 7-amino-4-methylcoumarin (AMC) was then measured at $\lambda_{ex} = 380$ nm and $\lambda_{em} = 435$ nm.

Apoptotic cellular morphology was assessed by Giemsa staining, performed according to a standard protocol. Briefly, cells were centrifuged, incubated with Giemsa for 15 min, and washed. Cells were mounted in Mowiol and examined using light microscopy. Photographs were taken with an RGB camera using Spot32 software and processed in PhotoShop. The intact nuclei of normal cells, which are stained blue, were easily distinguished from the condensed, fragmented, less intensely stained nuclei of apoptotic cells. Approximately 100 cells were evaluated per sample, and were scored as "apoptotic" or "normal" based on the presence or absence of condensed nuclei. Cell treatments were assessed in triplicate samples.

3. Results

3.1. Antiproliferative effects of the chelators

PIH, and two of its analogs, SIH and NIH, whose structures are shown in Fig. 1, were chosen for this study as they are among the best characterized of the many analogs synthesized in this laboratory [14]. Despite their structural similarity, their toxicities, as measured in a neuroblastoma cell line [10], range from the least toxic, PIH, to one of the most toxic, NIH.

PIH and two of its analogs evaluated in this study (Fig. 1) had antiproliferative effects on K562 cells (Fig. 2A), which were assessed after a 72-hr incubation. Concentration–response data, as measured by the MTS assay, were fitted

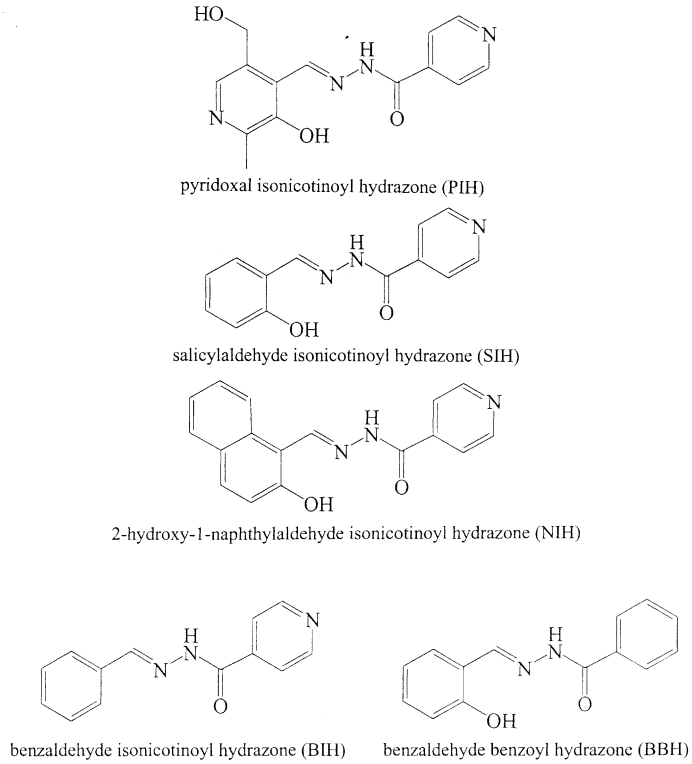

Fig. 1. Structures of the PIH analogs examined in this study.

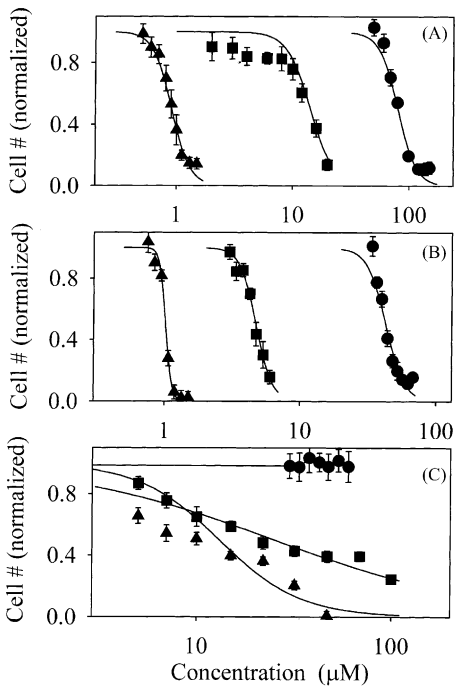

Fig. 2. Antiproliferative effects of PIH, SIH, NIH, and their Fe^{3+} complexes. Cells were incubated for 72 hr with PIH (●), SIH (■), NIH (▲), or their corresponding Fe^{3+} complexes. Cell viability was assessed spectrophotometrically, using the MTS assay. (A) K562 cells treated with chelators. (B) Jurkat cells treated with chelators. (C) Jurkat cells treated with iron-chelator complexes. Data points are the averages of six replicates that were normalized with respect to untreated cells, and the error bars represent standard deviations. Solid lines represent non-linear weighted least squares fits of the data to Eq. (1), except in the case of $FePIH_2$ treatment of Jurkat cells, which caused no cell death.

to a three-parameter logistic equation to obtain IC_{50} values, at which cell growth is half that of untreated cells ($Cells_{max}$):

$$\text{Relative cell number} = \frac{Cells_{max}}{(c/IC_{50})^b + 1} \quad (1)$$

in which c is the chelator concentration, and b is the Hill-type coefficient. PIH, which has been demonstrated to be well tolerated *in vivo* [8,9,12], had an IC_{50} of 90 μM, and was the least toxic, whereas the IC_{50} values of SIH and NIH were 12 and 1 μM, respectively.

The toxicity of PIH analogs toward Jurkat cells (Fig. 2B) was similar to the results obtained with K562 cells, although the IC_{50} values were approximately half those obtained using K562 cells, indicating the relative sensitivity of Jurkat cells to the toxic effects of the chelators. As was the case for neuroblastoma cells [10], toxicity of the chelators increased in the order PIH < SIH < NIH. This trend has been observed previously in K562 cells [17] and in a neuroblastoma cell line [10], and is consistent with the hypothesis that the toxicity of PIH analogs is correlated with their lipophilicity [17]. The antiproliferative effects of PIH, SIH, and NIH on Jurkat cells were time-dependent (Fig. 3).

3.2. Characterization of PIH analogs that do not mobilize iron

PIH analogs have been shown to have a number of effects on cells, including inhibition of transferrin-mediated

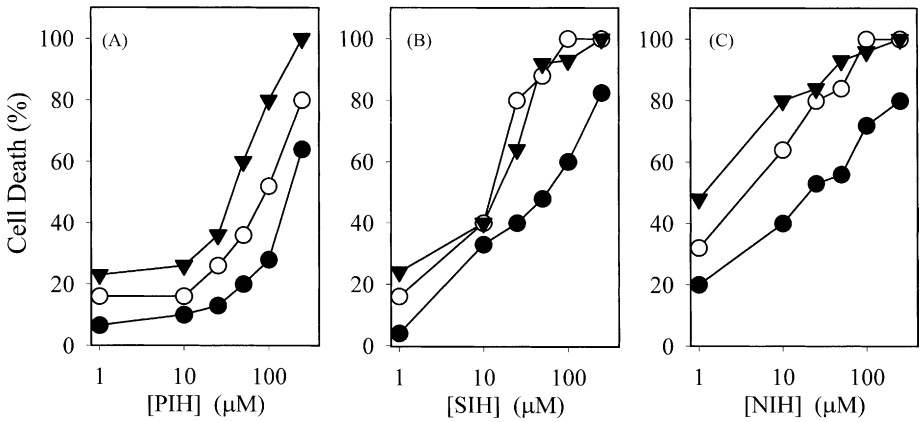

Fig. 3. Time- and concentration-dependence of PIH (A), SIH (B), and NIH (C) toxicity toward Jurkat cells. Cell death was assessed by trypan blue staining at 24 hr (●), 48 hr (○), and 72 hr (▼). Results shown are from a single experiment, which was performed twice.

iron uptake [10], inhibition of DNA synthesis [13], and mobilization of cellular iron [10,18], all of which have been explained by their direct interaction with iron. It is unknown, however, whether this class of iron chelators may cause toxicity via other biological effects. Two analogs, BIH and BBH, the structures of which are shown in Fig. 1, were synthesized. These compounds are similar to SIH, but lack the phenolic group that is essential for strong iron affinity, as demonstrated in X-ray crystallography [22], and by the shifts in infrared spectral bands that occur when PIH analogs bind iron [23]. That BIH and BBH do not bind iron was confirmed spectrophotometrically by the absence of ligand-to-metal charge transfer absorption, which is characteristic of PIH analogs [23,24].

The antiproliferative effects of BIH and BBH toward K562 cells were assessed over 72 hr, under conditions identical to those of Fig. 2A (data not shown). BIH, which was tested up to 1000 μM, was not toxic. The solubility limit of BBH was approximately 200 μM, below which no toxicity was observed. The toxicity of iron-citrate (prepared as described in Section 2) toward K562 cells was unaffected by the presence of 100 μM BIH or BBH (data not shown). Thus, it appears that the complete iron-binding motif, consisting of the phenolic oxygen, imine nitrogen, and carbonyl oxygen atoms, is necessary for the antiproliferative activity of PIH analogs.

3.3. ^{59}Fe mobilization from reticulocytes by PIH analogs

The capacity of iron chelators to mobilize intracellular iron was assessed using murine reticulocytes labeled with ^{59}Fe [18]. In this model, heme synthesis is inhibited by the incubation of reticulocytes with succinylacetone, which inhibits δ-aminolevulinic acid synthase, and $^{59}Fe_2$-transferrin, the biological iron donor. The efficacy of chelators at chelating intracellular iron and causing its release from cells may be evaluated in this system. PIH analogs have been studied using similar models [11], and the results agree well with the capacity of the chelators to cause the excretion of ^{59}Fe in rats [12]. PIH, SIH, and NIH bound ^{59}Fe in reticulocytes in which heme synthesis was inhibited with succinylacetone (Fig. 4); in this experiment the total ^{59}Fe taken up by the cells during the 1-hr incubation with $^{59}Fe_2$-transferrin corresponds to 100%. The amounts of ^{59}Fe bound by the chelators are represented by the total height of the bars, which are divided into ^{59}Fe released into the extracellular medium (dark shading) and intracellular, ethanol-soluble ^{59}Fe (light shading), which is presumably in the form of ^{59}Fe-chelator complexes.

As previously observed [24], PIH bound less ^{59}Fe than did its analogs. Although the total amounts of ^{59}Fe bound by SIH and NIH were high (Fig. 4), as is the case for most PIH analogs [24], the fraction remaining in the cell (light shading) was much higher than for the most effective analogs (approximately 1% under the same experimental conditions [24]). The accumulation of ^{59}Fe-chelator complexes in the cytosol, which appears to be due to the lipophilicity of the complexes [17], is correlated with toxicity, suggesting that intracellular iron-chelator complexes may have some cytotoxic effects.

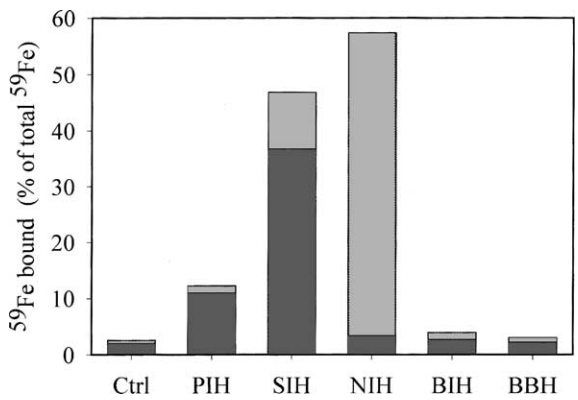

Fig. 4. Mobilization of ^{59}Fe from reticulocytes. Mouse reticulocytes were labeled with non-heme ^{59}Fe as described in Section 2 and incubated with 50 μM iron chelators for 2 hr. Dark bars represent ^{59}Fe bound and released into the extracellular medium, while light bars represent ^{59}Fe bound inside the cells. Data are expressed as a percentage of the total ^{59}Fe taken up by the cells during the labeling step. Data are the averages of triplicate samples, and standard deviations were not more than 2%.

As expected, neither BIH nor BBH bound significant amounts of ^{59}Fe (Fig. 4). It is unlikely that this is due to an inability of these compounds to penetrate the cell membrane, since their structures are similar to that of SIH, which readily crosses membranes to access ^{59}Fe (Fig. 4). Since these analogs do not bind iron strongly, they are unable to mobilize ^{59}Fe, and consequently have no antiproliferative effects. This strongly corroborates the hypothesis that iron binding is central to the biological activities of PIH analogs.

3.4. Iron chelators and apoptosis

The preceding experiments did not distinguish among the three mechanisms by which PIH analogs may affect cell growth: reduced growth rate, necrosis, and apoptosis. From the data in Fig. 3, concentrations of the chelators were chosen that caused significant antiproliferative effects: 100, 20, and 2 μM for PIH, SIH, and NIH, respectively. The death pathway taken by Jurkat cells was evaluated using two apoptotic markers: annexin-V binding, which measures phosphatidylserine externalization, and morphological evaluation following Giemsa staining. At all time points, the percentage of cells that were positive for markers of apoptosis was greater than or equal to that of dead cells (Fig. 5). Thus, at these concentrations of the chelators, apoptosis is the major, if not the only, mechanism of cell death triggered by PIH analogs.

Several other apoptotic and pro-apoptotic markers were evaluated after treatment of Jurkat cells with 100, 20, and 2 μM PIH, SIH, and NIH, respectively (Fig. 6). Mitochondrial destabilization, which occurs as a result of the opening of the mitochondrial permeability transition (MPT) pore, was measured using JC-1 [19], which shifts from red fluorescence to green when the mitochondrial potential drops below 100 mV, due to disaggregation of the dye. The percentage of cells containing green, destabilized mitochondria increased in a time-dependent manner (Fig. 6A).

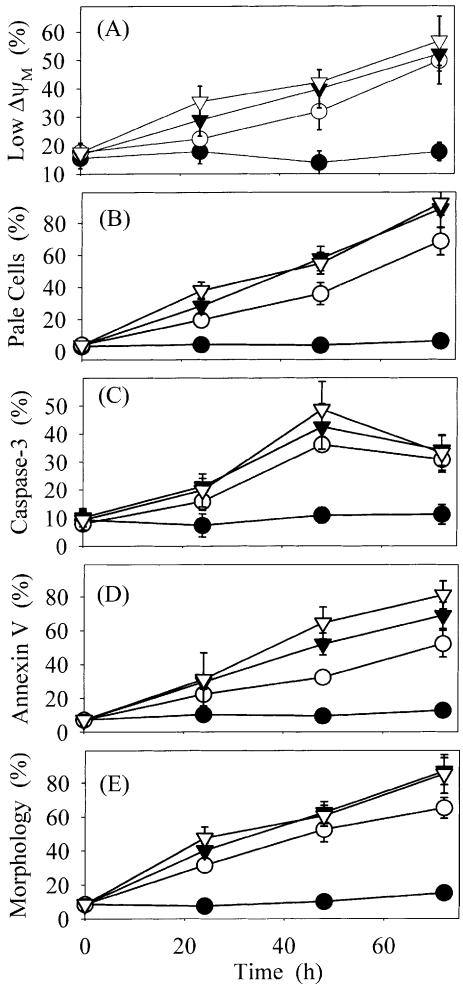

Fig. 6. Apoptosis induction in Jurkat cells by PIH analogs. Apoptosis was assessed in control cells (●), and at 100 μM PIH (○), 20 μM SIH (▼), and 2 μM NIH (▽) by measuring the collapse of the mitochondrial membrane potential ($\Delta\Psi_m$) with JC-1 (A), lysosomal destabilization with acridine orange (B), caspase-3 activity with Ac-DEVD-AMC (C), phosphatidylserine externalization with annexin-V-FITC (D), and morphological changes by Giemsa staining (E). Data points are the averages of three replicates, and error bars represent standard deviations. For some data points, error bars are smaller than the symbols.

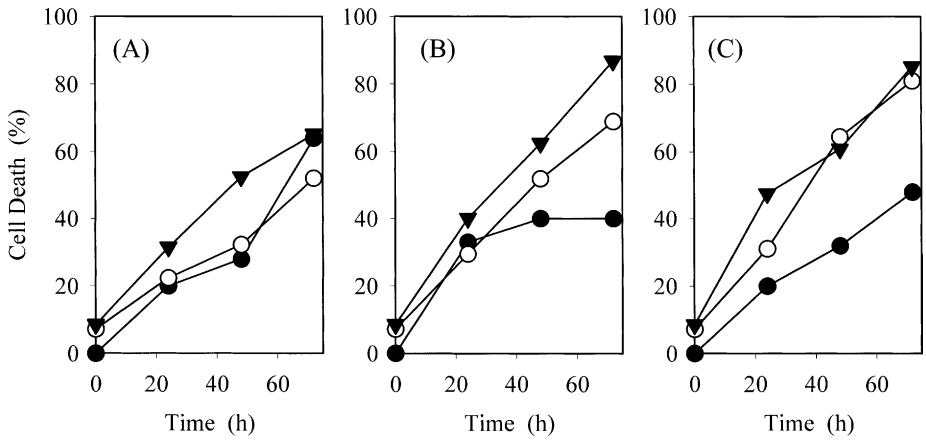

Fig. 5. Correlation of Jurkat cell death induced by PIH analogs with apoptosis markers. Cell death, assessed by trypan blue staining (●), phosphatidylserine externalization, assessed by annexin-V-FITC binding (○), and morphological changes, assessed by Giemsa staining (▼), were measured over time at 100 μM PIH (A), 20 μM SIH (B), and 2 μM NIH (C). Data shown are from a single experiment, which was performed three times.

The fluorophore AO is a weak base that accumulates in the acidic environment of the lysosome. A decrease in AO fluorescence, detectable by flow cytometry, indicates the loss of the lysosomal proton gradient [25], and is thus a marker of lysosomal membrane integrity. Incubation of Jurkat cells with PIH analogs resulted in a significant increase in the number of "pale cells," indicating that these chelators cause lysosomal destabilization (Fig. 6B). Other cytotoxic stimuli also have this effect on lysosomes, including the redox-cycling quinone, naphthazirin [26], the lysosome-specific detergent MSDH [27], lysosomally targeted photo-oxidative damage [28], and Fas/APO-1 [29].

Similar effects of chelators on K562 cells were observed for all apoptotic markers (Fig. 7), although the extent of apoptosis was generally lower, due to the greater resistance of these cells to the antiproliferative effects of these chelators (Fig. 2). Because they had similar effects on two different cell lines, the observed induction of apoptosis by the chelators is likely to be a general effect on different cell types.

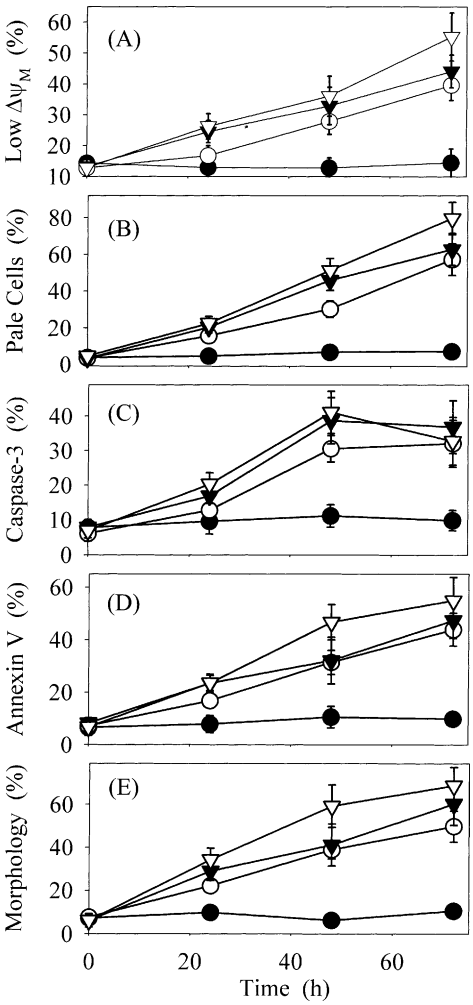

Fig. 7. Apoptosis induction in K562 cells by PIH analogs. Apoptosis was assessed in control cells (●), and at 100 μM PIH (○), 20 μM SIH (▼), and 2 μM NIH (▽) by measuring the collapse of the mitochondrial membrane potential ($\Delta\Psi_m$) with JC-1 (A), lysosomal destabilization with acridine orange (B), caspase-3 activity with Ac-DEVD-AMC (C), phosphatidylserine externalization with annexin-V-FITC (D), and morphological changes by Giemsa staining (E). Data points are the averages of three replicates, and error bars represent standard deviations. For some data points, error bars are smaller than the symbols.

The sequence of events in the apoptotic cascade was probed by assessing various markers of apoptosis in the presence and absence of the pan-caspase inhibitor zVAD-fmk (Fig. 8). At equitoxic concentrations, all analogs had similar effects on both cell lines after a 48-hr incubation. As was shown in Figs. 6 and 7 for Jurkat and K562 cells, respectively, incubation of cells with PIH analogs caused mitochondrial and lysosomal destabilization, caspase-3 activation, phosphatidylserine externalization, and morphological changes associated with apoptosis (Fig. 8). In the presence of the caspase inhibitor zVAD-fmk, lysosomal and mitochondrial effects were unchanged (Student's *t*-test, $P > 0.05$ in all cases), indicating that these events occur upstream of caspase activation. Phosphatidylserine externalization and morphological alterations, however, were inhibited significantly by zVAD-fmk: $P < 0.05$ in all cases except for the assessment of K562 cells with SIH, in which the *P*-value for phosphatidylserine externalization was 0.051. One explanation for these observations is that these events are caspase-dependent, and therefore occur downstream of caspase activation in both Jurkat and K562 cells. However, 25 μM zVAD-fmk was unable to protect Jurkat cells from the toxicity of PIH analogs over a 72-hr incubation (data not shown). Therefore, it is possible that apoptosis may proceed through multiple mechanisms, including a caspase-independent pathway such as apoptosis-inducing factor [30], or that in the absence of caspase activity damaged cells die by necrosis.

To further characterize the pathway by which apoptosis is induced in response to PIH analogs, Jurkat cells transfected with CrmA [15], an inhibitor of caspase-8 [31], were examined. As a positive control, the inhibitory effect of CrmA overexpression on apoptosis induced by anti-Fas IgM was confirmed (Fig. 9). Wild-type Jurkat cells were sensitive to apoptosis induced by anti-Fas IgM; 68 ± 7% of the cells were annexin-positive, whereas apoptosis in CrmA-overexpressing cells was almost completely inhibited. In contrast, the extent of apoptosis induced by PIH, SIH, or NIH in CrmA-overexpressing cells was not significantly different from that in control cells (Fig. 9). Thus, as is the case for many chemical inducers of apoptosis, the main pro-apoptotic pathway appears to be independent of caspase-8.

Jurkat cells overexpressing Bcl-2 [15], an anti-apoptotic mitochondrial protein [32], were partially protected against anti-Fas, IgM-induced apoptosis. This cell line was also relatively resistant to apoptosis induced by PIH, SIH, and NIH (Fig. 9); approximately 45% of wild-type cells were annexin-positive, as compared to approximately 17% of Bcl-2 overexpressing cells. This effect of Bcl-2 demonstrates the importance of mitochondria in the pathway of apoptosis induced by PIH analogs.

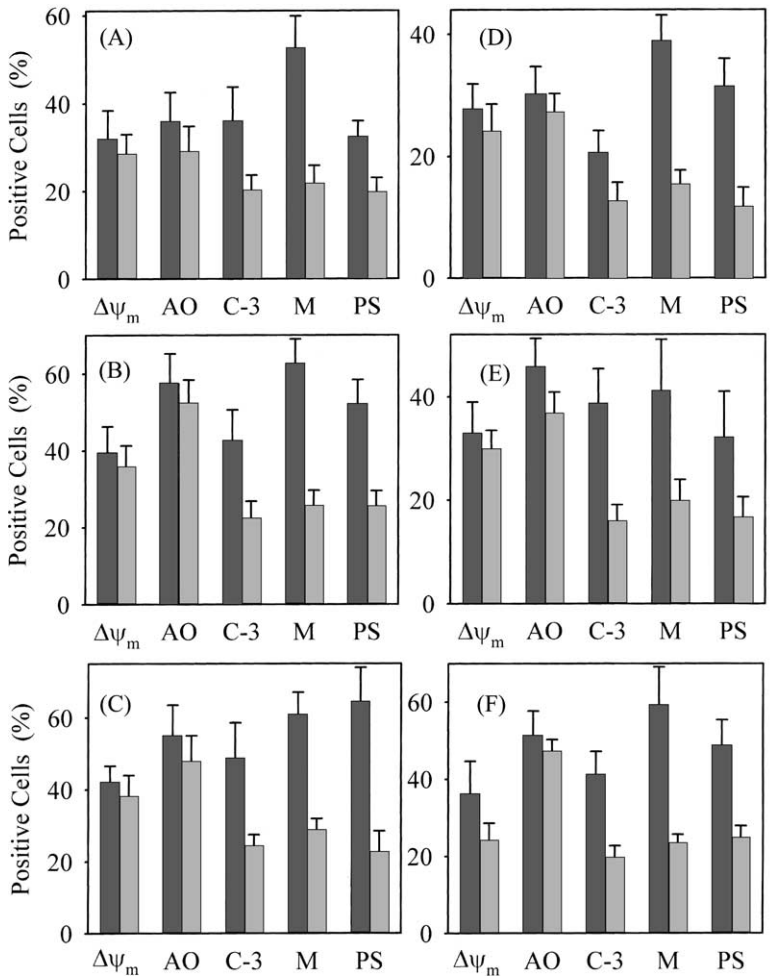

Fig. 8. Effect of zVAD-fmk on the inhibition of apoptotic events induced by PIH analogs. Jurkat (A–C) and K562 (D–F) cells were incubated for 48 hr with 100 μM PIH (A and D), 20 μM SIH (B and E), and 2 μM NIH (C and F) in the absence (dark bars) and presence (light bars) of 25 μM zVAD-fmk. The following apoptotic markers were assessed: loss of the mitochondrial membrane potential ($\Delta\Psi_m$), lysosomal destabilization (AO), caspase-3 activity (C-3), morphological changes (M), and phosphatidylserine externalization (PS). The data represent the averages of three replicates, and the error bars represent standard deviations. In no case was $\Delta\Psi_m$ or AO significantly different in the presence and absence of zVAD-fmk. C-3, M, and PS were significantly different ($P < 0.05$) in each case, except in E, in which $P = 0.051$ (Student's *t*-test) for PS.

3.5. Apoptosis induction by Fe^{3+}-chelator complexes

Toxicity of the iron-chelator complexes was assessed in Jurkat cells (Fig. 2C), and analyzed as described for the free chelators. Toxicity of $FePIH_2$ was not observed below its solubility limit (approximately 150 μM). $FeSIH_2$ and $FeNIH_2$ were toxic, with IC_{50} values of 77 ± 5 and 85 ± 7 μM, respectively. That incubation of Jurkat cells with $FeSIH_2$ and $FeNIH_2$ induced apoptosis in a time- and concentration-dependent manner, as assessed by annexin-V binding, is shown in Table 1. Caspase activation paralleled annexin-V binding (data not shown). As expected from the lack of toxicity of $FePIH_2$ toward Jurkat cells (Fig. 2C), $FePIH_2$ did not induce apoptosis at any concentration.

Evidence for a contribution to the toxicity of PIH analogs by their iron complexes is demonstrated in Fig. 10, which shows the protective effect of BSA against the toxicity of PIH, SIH, and NIH. PIH analogs bind

Table 1
Induction of apoptosis by the Fe^{3+} complexes of PIH analogs

	Phosphatidylserine externalization[a] (%)		
	24 hr	48 hr	66 hr
Control[b]	8.2 ± 5.1	7.2 ± 1.2	12.3 ± 4.1
37.5 μM $FePIH_2$[c]	13.2 ± 2.8	10.8 ± 2.1	13.1 ± 3.2
75 μM $FePIH_2$[c]	12.1 ± 3.5	11.2 ± 2.5	12.9 ± 3.7
37.5 μM $FeSIH_2$	17.1 ± 2.1	11.8 ± 2.3	15.2 ± 4.1
75 μM $FeSIH_2$	16.2 ± 4.1	15.1 ± 4.2	16.5 ± 2.9
150 μM $FeSIH_2$			53.9 ± 1.8[d]
37.5 μM $FeNIH_2$	9.9 ± 4.2	15.2 ± 3.8	28.9 ± 4.2
75 μM $FeNIH_2$	21.3 ± 5.8	47.2 ± 4.9	62.2 ± 7.2
150 μM $FeNIH_2$			92.0 ± 0.2[d]

[a] Jurkat cells were incubated with Fe^{3+} complexes of the ligands at the indicated concentrations. Annexin-V-FITC binding and caspase activation were assessed by flow cytometry as described in Section 2. Values are averages of triplicate measurements, and errors are standard deviations.

[b] Annexin binding for control cells at time zero was 7.5 ± 3.5%.

[c] Concentrations are indicated in terms of Fe.

[d] These data are from a separate experiment, in which caspase activation was not assessed.

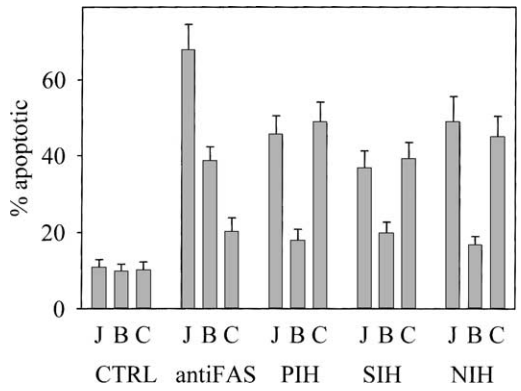

Fig. 9. Roles of caspase-8 and Bcl-2 in apoptosis induced by PIH analogs. Jurkat cells (J) overexpressing Bcl-2 (B) or the caspase-8 inhibitor CrmA (C) were exposed to anti-Fas IgM, 100 μM PIH, 20 μM SIH, and 2 μM NIH for 48 hr. Apoptosis was assessed by phosphatidylserine externalization. Data represent averages of three replicates, and error bars represent standard deviations. There was no significant difference among the cell lines in the absence of the apoptogenic agent. CrmA and Bcl-2 overexpression significantly protected Jurkat cells against anti-Fas IgM-induced apoptosis ($P < 0.05$, one-tailed t-test). Bcl-2 overexpression significantly protected cells against PIH analog-induced apoptosis ($P < 0.05$, one-tailed t-test), whereas CrmA overexpression had no effect.

intracellular iron, resulting in the transient accumulation of iron-chelator complexes inside cells [24], as shown in Fig. 4. The rate of diffusion of the complexes through the cell membrane into the extracellular medium determines the intracellular concentration of iron-chelator [17]. Because of its high affinity for iron-chelator complexes [24], the addition of BSA to the extracellular medium enhances the release of ^{59}Fe-chelator complexes from the cell, and therefore reduces the accumulation of intracellular ^{59}Fe-chelator [24]. This effect caused a significant decrease in the toxicity of PIH analogs, as shown in Fig. 10. Thus, the toxicity of PIH analogs is due, in part, to the toxicity of the iron-chelator complexes that are formed intracellularly.

4. Discussion

4.1. Relationship of the toxicity of PIH analogs to interaction with intracellular iron

The hypothesis that the biological effects of PIH and its analogs are related to their effects on cellular iron was tested by synthesizing and evaluating the effects of BIH and BBH, PIH analogs that do not bind iron. These ligands were designed to be as similar as possible to SIH, which enters reticulocytes readily and binds intracellular ^{59}Fe (Fig. 4), and activates protein-1 IRP-1 in the macrophage cell line RAW 264.7 [33]. Its Fe^{3+} complex [34], as well as that of PIH [35], delivers iron to cells, supporting cell growth in the absence of transferrin, the biological iron donor. No interaction of BIH or BBH with iron was observed, either spectrophotometrically (data not shown) or in the reticulocyte ^{59}Fe mobilization assay (Fig. 4). The structural changes that abrogated iron affinity also abolished toxicity toward K562 cells. These data demonstrate that, as hypothesized, iron binding is central to the activity of PIH analogs.

4.2. PIH analog-induced apoptosis via mitochondrial damage

The toxicity results of PIH, SIH, and NIH in Jurkat T lymphocytes and K562 cells found in this study (Fig. 2) are consistent with the results of a study describing the toxicity of PIH analogs as assessed in a neuroblastoma cell line [10], in that SIH and NIH had much stronger antiproliferative effects than did PIH. CrmA overexpression did not affect the toxicity of PIH analogs (Fig. 9), suggesting that caspase-8, involved in receptor-mediated apoptosis [36], does not play a significant role in the induction of apoptosis by these chelators. Bcl-2 overexpression, on the other hand, inhibited the progression of chelator-induced apoptosis

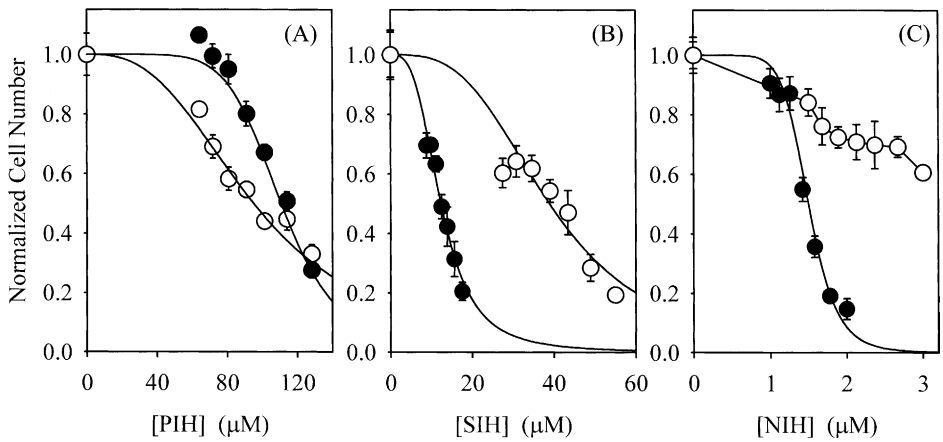

Fig. 10. Effect of BSA on the toxicity of PIH analogs toward K562 cells. Cells were exposed to PIH (A), SIH (B), and NIH (C) in the absence (●) and presence (○) of 5% BSA for 72 hr. Cell viability was assessed using the MTS assay. Data points represent the averages of six replicates, and the error bars represent standard deviations. Solid lines represent non-linear weighted least squares fits of the data to Eq. (1), except for the treatment with NIH and BSA; in this case cell viability in the presence of 3 μM NIH was greater than 0.5.

significantly (Fig. 9). Bcl-2 appears to protect cells against mitochondrially-mediated apoptosis [32] through a balance of pro- and anti-apoptotic factors. Thus, protection by Bcl-2 against apoptosis induced by PIH analogs supports the hypothesis that they act by damaging mitochondria, which then causes caspase activation.

Treatment of Jurkat and K562 cells with PIH analogs caused apoptosis in which lysosomal and mitochondrial destabilization occurred upstream of, or independently of, caspase activation, whereas phosphatidylserine externalization and development of apoptotic morphology were inhibited by the caspase inhibitor zVAD-fmk (Fig. 8). This sequence of events is consistent with the ''mitochondrial'' pathway of apoptosis [36], in which mitochondrial damage causes cytochrome *c* release and caspase activation, which result in cell death. Together with the protection by Bcl-2 against PIH-induced apoptosis (Fig. 9), these data support a mechanism of action in which mitochondrial damage and subsequent cytochrome *c* release cause caspase activation. However, since caspase inhibition by zVAD-fmk was unable to protect Jurkat cells against the toxicity of the PIH analogs $FeSIH_2$ or $FeNIH_2$ (data not shown), the possibility that cells die through multiple mechanisms must be considered.

An early event in apoptosis induced by PIH analogs was lysosomal destabilization (Fig. 8), which has also been observed in apoptosis mediated by a number of diverse stimuli: Fas/APO-1 [29], MSDH [27], and oxidants including photo-oxidation [28] and naphthazirin [26,27]. Time–course studies have demonstrated that lysosomal destabilization is one of the earliest detectable events, involving the loss of the proton gradient followed by leakage of lysosomal contents [28], and occurring prior to loss of the mitochondrial membrane potential [37].

4.3. Apoptosis induction by iron-chelator complexes

Treatment of Jurkat T cells with the Fe^{3+} complexes of PIH, SIH, and NIH caused cell death (Fig. 2C), as previously reported in other cell lines for $FePIH_2$ [38,39] and the Fe^{3+} complexes of other PIH analogs, including SIH and NIH [17]. Although under the experimental conditions described, $FePIH_2$ was not toxic below its solubility limit, the IC_{50} values of $FeSIH_2$ and $FeNIH_2$ were approximately 77 and 85 μM for Jurkat T cells (Fig. 2C), respectively, values far higher than those of the free ligands (Fig. 2). As was the case for the free chelators, the Fe^{3+} complexes caused apoptosis (Table 1). In contrast to the present findings, a previous study found that the Fe^{3+} complex of NIH, formed in a 1:1 ratio, had no antiproliferative effects toward SK-N-MC cells below 50 μM [40], which may be the result of the relative resistance of this cell line, or a consequence of the difference in the stoichiometry of the complex. The mechanism by which iron complexes of PIH analogs cause toxicity is unknown, but may be related to their capacity to deliver iron to cells; FePIH, at concentrations below 1 μM, delivered iron to proliferating mouse lymphocytes in an apparently non-specific manner [41], resulting in the accumulation of iron in pools that had escaped or overloaded the normal intracellular iron trafficking pathways. Non-specific iron delivery may inappropriately regulate biochemical processes that are sensitive to intracellular iron levels and/or oxidative stress, such as the IRP system [33] or cyclin-dependent kinases [42].

4.4. Mechanisms of toxicity of PIH analogs

The capacity of PIH analogs to mobilize iron *in vitro* [10,11] and *in vivo* [8,12] is well characterized, and iron chelation may contribute to the toxicity of PIH analogs by depleting cells of the iron they require for proliferation. However, iron depletion cannot be the only mechanism by which PIH analogs are toxic. The capacity of PIH analogs, aside from PIH itself, which was significantly less effective than all the analogs tested, to bind ^{59}Fe in ^{59}Fe-labeled reticulocytes and K562 cells was similar [24] (although there were great differences in the capacity of the analogs to efflux the ^{59}Fe), whereas the toxicity of these analogs varied over two orders of magnitude [17]. Furthermore, ^{59}Fe mobilization from K562 cells reaches a maximum level at 10 μM for all the chelators tested [17], whereas the toxicity of some PIH analogs is not observed until much higher concentrations are reached. Thus, the effect of diverting iron from its normal cellular ligands, while it may contribute to the overall toxicity observed, is insufficient to account for either the observed antiproliferative effects, or the structure–activity relationships governing the toxicity of this class of chelators.

The main factor that correlated with the toxicity of PIH analogs is their lipophilicity, which has been the focus of a number of studies [17,24,43,44]. PIH analogs appear to enter cells with ease, as demonstrated by their similar capacity to bind cellular ^{59}Fe [24]. Thus, the role of lipophilicity in determining toxicity is unlikely to be due to the membrane permeability of the chelators. Toxicity is correlated with high lipophilicity of the Fe^{3+} complexes of PIH analogs, which inhibits their release from the cell [17]. Thus, the simplest explanation for the observed structure–activity relationships is that the intracellular concentration of the iron-chelator, at least in part, determines the toxicity. In support of this hypothesis is the protective effect of BSA against the toxicity of PIH analogs (Fig. 10). BSA binds Fe^{3+} complexes of PIH analogs tightly, and improves iron mobilization by PIH analogs in reticulocytes and K562 cells [24]. BSA presumably acts by providing an extracellular sink for the lipophilic iron complexes. BSA, at its plasma concentration, also diminishes the toxicity of all PIH analogs tested in K562 cells (Fig. 10, [17]). This is apparently the result of the reduction of intracellular levels of the iron complexes, which occurs because BSA expedites their

release from the cell [17]. This observation is a strong argument for the hypothesis that accumulation of iron complexes in the cell is, at least in part, the cause of the toxicity induced by PIH analogs.

Acknowledgments

The financial assistance of the CIHR, in the form of operating funds, and of the National Cooley's Anemia Foundation, in the form of a postdoctoral fellowship (J.L.B.), is gratefully acknowledged. J.N. was partially supported by a University of Linköping Grant (83081030).

References

[1] Ponka P, Beaumont C, Richardson DR. Function and regulation of transferrin and ferritin. Semin Hematol 1998;35:35–54.
[2] Hileti D, Panayiotidis P, Hoffbrand AV. Iron chelators induce apoptosis in proliferating cells. Br J Haematol 1995;89:181–7.
[3] Tanaka T, Satoh T, Onozawa Y, Kohroki J, Itoh N, Ishidate Jr M, Muto N, Tanaka K. Apoptosis during iron-chelator-induced differentiation in F9 embryonal carcinoma cells. Cell Biol Int 1999;23:541–50.
[4] Juckett MB, Shadley JD, Zheng Y, Klein JP. Desferrioxamine enhances the effects of gamma radiation on clonogenic survival and the formation of chromosomal aberrations in endothelial cells. Radiat Res 1998;149:330–7.
[5] Rakba N, Loyer P, Gilot D, Delcros JG, Glaise D, Baret P, Pierre JL, Brissot P, Lescoat G. Antiproliferative and apoptotic effects of *O*-Trensox, a new synthetic iron-chelator, on differentiated human hepatoma cell lines. Carcinogenesis 2000;21:943–51.
[6] Simonart T, Degraef C, Andrei G, Mosselmans R, Hermans P, Van Vooren JP, Noel JC, Boelaert JR, Snoeck R, Heenen M. Iron chelators inhibit the growth and induce the apoptosis of Kaposi's sarcoma cells and of their putative endothelial precursors. J Invest Dermatol 2000;115:893–900.
[7] Brittenham GM. Pyridoxal isonicotinoyl hydrazone. Effective iron-chelation after oral administration. Ann NY Acad Sci 1990;612: 315–26.
[8] Cikrt M, Ponka P, Necas E, Neuwirt J. Biliary iron excretion in rats following pyridoxal isonicotinoyl hydrazone. Br J Haematol 1980; 45:275–83.
[9] Sookvanichsilp N, Nakornchai S, Weerapradist W. Toxicological study of pyridoxal isonicotinoyl hydrazone: acute and subchronic toxicity. Drug Chem Toxicol 1991;14:395–403.
[10] Richardson DR, Tran EH, Ponka P. The potential of iron chelators of the pyridoxal isonicotinoyl hydrazone class as effective antiproliferative agents. Blood 1995;86:4295–306.
[11] Ponka P, Baker E, Edward JT. Effect of pyridoxal isonicotinoyl hydrazone and other hydrazones on iron release from macrophages, reticulocytes and hepatocytes. Biochim Biophys Acta 1988;967: 122–9.
[12] Blaha K, Cikrt M, Nerudova J, Fornuskova H, Ponka P. Biliary iron excretion in rats following treatment with analogs of pyridoxal isonicotinoyl hydrazone. Blood 1998;91:4368–72.
[13] Richardson DR, Ponka P. The iron metabolism of the human neuroblastoma cell: lack of relationship between the efficacy of iron-chelation and the inhibition of DNA synthesis. J Lab Clin Med 1994;124: 660–71.
[14] Edward JT, Gauthier M, Chubb FL, Ponka P. Synthesis of new acylhydrazones as iron-chelating compounds. J Chem Eng Data 1988;33:538–40.
[15] Hockenbery DM, Oltvai ZN, Yin XM, Milliman CL, Korsmeyer SJ. Bcl-2 functions in an anti-oxidant pathway to prevent apoptosis. Cell 1993;75:241–51.
[16] Gamen S, Anel A, Perez-Galan P, Lasierra P, Johnson D, Pineiro A, Naval J. Doxorubicin treatment activates a Z-VAD-sensitive caspase, which causes deltapsim loss, caspase-9 activity, and apoptosis in Jurkat cells. Exp Cell Res 2000;258:223–35.
[17] Buss JL, Arduini E, Shephard KC, Ponka P. Lipophilicity of analogs of pyridoxal isonicotinoyl hydrazone (PIH) determines efflux of Fe complexes and toxicity in K562 cells. Biochem Pharmacol, in press.
[18] Huang AR, Ponka P. A study of the mechanism of action of pyridoxal isonicotinoyl hydrazone at the cellular level using reticulocytes loaded with non-heme ^{59}Fe. Biochim Biophys Acta 1983;757:306–15.
[19] Neuzil J, Svensson I, Weber T, Weber C, Brunk UT. α-Tocopheryl succinate-induced apoptosis in Jurkat T cells involves caspase-3 activation, and both lysosomal and mitochondrial destabilisation. FEBS Lett 1999;445:295–300.
[20] Neuzil J, Weber T, Schröder A, Lu M, Ostermann G, Gellert N, Mayne GC, Olejnicka B, Nègre-Salvayre A, Stícha M, Coffey RJ, Weber C. Induction of cancer cell apoptosis by α-tocopheryl succinate: molecular pathways and structural requirements. FASEB J 2001;15:403–15.
[21] Neuzil J, Schroder A, von Hundelshausen P, Zernecke A, Weber T, Gellert N, Weber C. Inhibition of inflammatory endothelial responses by a pathway involving caspase activation and p65 cleavage. Biochemistry 2001;40:4686–92.
[22] Murphy TB, Johnson DK, Rose NJ, Aruffo A, Schomaker V. Structural studies of iron(III) complexes of the new iron-binding drug, pyridoxal isonicotinoyl hydrazone. Inorg Chim Acta 1982;66:L67–8.
[23] Ponka P, Grady RW, Wilczynska A, Schulman HM. The effect of various chelating agents on the mobilization of iron from reticulocytes in the presence and absence of pyridoxal isonicotinoyl hydrazone. Biochim Biophys Acta 1984;802:477–89.
[24] Buss JL, Arduini E, Ponka P. Mobilization of intracellular iron by analogs of pyridoxal isonicotinoyl hydrazone (PIH) is determined by the membrane permeability of the iron-chelator complexes. Biochem Pharmacol 2002;64:1689–701.
[25] Brunk UT, Svensson I. Oxidative stress, growth factor starvation and Fas activation may all cause apoptosis through lysosomal leak. Redox Rep 1999;4:3–11.
[26] Roberg K, Ollinger K. Oxidative stress causes relocation of the lysosomal enzyme cathepsin D with ensuing apoptosis in neonatal rat cardiomyocytes. Am J Pathol 1998;152:1151–6.
[27] Li W, Yuan X, Nordgren G, Dalen H, Dubowchik GM, Firestone RA, Brunk UT. Induction of cell death by the lysosomotropic detergent MSDH. FEBS Lett 2000;470:35–9.
[28] Brunk UT, Dalen H, Roberg K, Hellquist HB. Photo-oxidative disruption of lysosomal membranes causes apoptosis of cultured human fibroblasts. Free Radic Biol Med 1997;23:616–26.
[29] Deiss LP, Galinka H, Berissi H, Cohen O, Kimchi A. Cathepsin D protease mediates programmed cell death induced by interferon-γ, Fas/APO-1 and TNF-α. EMBO J 1996;15:3861–70.
[30] Susin SA, Lorenzo HK, Zamzami N, Marzo I, Snow BE, Brothers GM, Mangion J, Jacotot E, Costantini P, Loeffler M, Larochette N, Goodlett DR, Aebersold R, Siderovski DP, Penninger JM, Kroemer G. Molecular characterization of mitochondrial apoptosis-inducing factor. Nature 1999;397:441–6.
[31] Zhou Q, Snipas S, Orth K, Muzio M, Dixit VM, Salvesen GS. Target protease specificity of the viral serpin CrmA. Analysis of five caspases. J Biol Chem 1997;272:7797–800.
[32] Hockenbery D, Nunez G, Milliman C, Schreiber RD, Korsmeyer SJ. Bcl-2 is an inner mitochondrial membrane protein that blocks programmed cell death. Nature 1990;348:334–6.
[33] Kim S, Ponka P. Effects of interferon-γ and lipopolysaccharide on macrophage iron metabolism are mediated by nitric oxide-induced degradation of iron regulatory protein 2. J Biol Chem 2000;275: 6220–6.

[34] Laskey J, Webb I, Schulman HM, Ponka P. Evidence that transferrin supports cell proliferation by supplying iron for DNA synthesis. Exp Cell Res 1988;176:87–95.
[35] Ponka P, Schulman HM, Wilczynska A. Ferric pyridoxal isonicotinoyl hydrazone can provide iron for heme synthesis in reticulocytes. Biochim Biophys Acta 1982;718:151–6.
[36] Hengartner MO. The biochemistry of apoptosis. Nature 2000;407: 770–6.
[37] Roberg K, Johansson U, Öllinger K. Lysosomal release of cathepsin D precedes relocation of cytochrome *c* and loss of mitochondrial transmembrane potential during apoptosis induced by oxidative stress. Free Radic Biol Med 1999;27:1228–37.
[38] Tsao MS, Sanders GH, Grisham JW. Regulation of growth of cultured hepatic epithelial cells by transferrin. Exp Cell Res 1987;171:52–62.
[39] Brock JH, Stevenson J. Replacement of transferrin in serum-free cultures of mitogen-stimulated mouse lymphocytes by a lipophilic iron-chelator. Immunol Lett 1986;15:23–5.
[40] Richardson DR, Bernhardt PV. Crystal and molecular structure of 2-hydroxy-1-naphthylaldehyde isonicotinoyl hydrazone (NIH) and its iron(III) complex: an iron-chelator with anti-tumour activity. J Biol Inorg Chem 1999;4:266–73.
[41] Djeha A, Brock JH. Uptake and intracellular handling of iron from transferrin and iron chelates by mitogen stimulated mouse lymphocytes. Biochim Biophys Acta 1992;1133:147–52.
[42] Darnell G, Richardson DR. The potential of iron chelators of the pyridoxal isonicotinoyl hydrazone class as effective antiproliferative agents III: the effect of the ligands on molecular targets involved in proliferation. Blood 1999;94:781–92.
[43] Edward JT, Chubb FL, Sangster J. Iron chelators of the pyridoxal isonicotinoyl hydrazone class. Relationship of the lipophilicity of the apochelator to its ability to mobilize iron from reticulocytes in vitro: reappraisal of reported partition coefficients. Can J Physiol Pharmacol 1997;75:1362–8.
[44] Ponka P, Richardson DR, Edward JT, Chubb FL. Iron chelators of the pyridoxal isonicotinoyl hydrazone class. Relationship of the lipophilicity of the apochelator to its ability to mobilise iron from reticulocytes in vitro. Can J Physiol Pharmacol 1994;72: 659–66.